International Journal of Pharmaceutics 361 (2008) 150–157

Contents lists available at ScienceDirect

International Journal of Pharmaceutics

journal homepage: www.elsevier.com/locate/ijpharm

Evaluation of dynamic image analysis for characterizing pharmaceutical excipient particles

Weili Yu*, Bruno C. Hancock

Pfizer Global Research and Development, Eastern Point Road, MS 8156-007, Groton, CT 06340, USA

ARTICLE INFO

Article history:
Received 27 February 2008
Received in revised form 23 May 2008
Accepted 26 May 2008
Available online 23 June 2008

Keywords:
Dynamic image analysis
QicPic
Particle size
Particle shape
Laser diffraction
Microcrystalline cellulose

ABSTRACT

The capability of the newly developed dynamic image analysis instrument QicPic equipped with the high-speed dry-powder-dispersing device was investigated systematically using various MCC particles. Instrument cross-validation was conducted by comparing the particle size distribution of spherical particles obtained with the QicPic and with a conventional laser diffraction instrument (HELOS). While good agreement was observed with spherical particles, significant differences were found when analyzing rod-shaped Ceolus™ KG-1000 particles, revealing the intrinsic difference in operating principles between these two techniques. Particle shape distributions of several spherical and rod-shaped samples obtained with the QicPic were compared to scanning electron micrographs (SEMs), and semi-quantitative agreement was obtained. The particle size and particle shape of a series of binary particulate systems composed of both spherical (CP-102) and rod-shaped (KG-1000) particles of varying mass ratios were analyzed using the QicPic. The particle size and shape distributions of these binary mixtures were also computed using the distributions of the pure components weighted by their respective mass fractions. Comparisons between the measured and computed distributions appeared to indicate that the QicPic overestimated the amount of KG-1000 particles present in all the mixtures. Further analysis revealed that the observed discrepancy might be caused by a particle porosity effect.

1. Introduction

The particle size of pharmaceutical materials has attracted much attention due to its reported impact on drug bioavailability and the manufacturability of various dosage forms, whereas much less attention has been given to the impact of particle shape (Hintz and Johnson, 1989; Fee et al., 1992; Johnson and Swindell, 1996; Podczeck and Sharma, 1996; Zhang and Johnson, 1997; Massol-Chaudeur et al., 2002; Swaminathan and Kildsig, 2002; Mullarney et al., 2003; Yin et al., 2005; Shah et al., 2007). One of the reasons for this is the lack of suitable technologies for reliable quantitative particle shape characterization. Attempts have been made to expand the capability of conventional laser diffraction technique to include particle shape analysis, but only limited success has been achieved so far (Ma et al., 2001; Deriemaeker and Finsy, 2005). Image analysis (IA) is probably still the most frequently used technique for characterizing particle shape (Bao et al., 2004; Li et al., 2005), but until recently, the level of automation for image analysis remained low, and manual operation was required for sample preparation, measurement and data analysis. This was often tedious and time consuming, and the number of particles analyzed was relatively small, resulting in significant statistical errors. Masuda and Iinoya proposed a mathematical procedure for estimating the number of particles to be counted for image analysis to keep errors associated with size determination within a desired range (Masuda and Iinoya, 1971). Jillavenkatesa et al. used this procedure and estimated that for a log-normal distribution with a variance of 0.2209, approximately 3400 particles need to be analyzed to have 99% of the data lie within ±5% of relative error (Jillavenkatesa et al., 2001).

Recent advances in high-speed digital camera and computer technologies have enabled the development of automated image analysis instrumentations that are capable of capturing two-dimensional images of particles that are either stationary (SIA) or mobile (DIA) when presented in front of the detector. For SIA, a thin layer of particles (in air or emerged in a liquid) is placed on a (glass) slide and presented to the focal plan of a microscope so that images of particles can be captured. The number of particles per measurement is typically fixed and is limited by the size of the slide used for sample presentation. Dynamic image analysis (DIA) allows measurements of particles in motion (Xu et al., 2003; Rabinski and Thomas, 2004). In contrast to SIA where particles are positioned manually at the focal plane of the microscope, particles in a DIA system are distributed within a finite depth defined by the design of the instrument. To minimize the effect of out-of-focus images,

* Corresponding author. Tel.: +1 860 686 2072; fax: +1 860 686 5632.
E-mail address: Weili.yu@pfizer.com (W. Yu).

0378-5173/$ – see front matter © 2008 Elsevier B.V. All rights reserved.
doi:10.1016/j.ijpharm.2008.05.025

several approaches have been taken, including using a sheath flow cell to transform particle suspension to a flat flow (Malvern Sysmax FPIA 300), use of a telecentric optic design to extend focusing volume up to 3 mm in length (Beckman Coulter RapidVUE), and applying compensation factors based on statistical models to each image frame (Rabinski and Thomas, 2004). Most of the DIA systems have been limited to wet analysis, where particles are suspended in a liquid medium to allow easy control of particle flow rate and thus reduction of motion blur during image acquisition.

Recently, Sympatec Inc. (Clausthal-Zellerfeld, Germany) have developed and commercialized a DIA system (QicPic) that is capable of capturing images of dry powder particles in a fast moving air stream (Witt et al., 2004, 2005; Köhler et al., 2007). During the analysis, dry powder particles are first placed on a vibratory chute and then accelerated to a high speed by a Venturi tube located in the sample dispersion line. Images of the particles are captured by a high-speed digital camera with a synchronized light source. To obtain images with sufficient optical contrast, an aperture stop is used with the imaging objectives to allow only light rays parallel to the optical axis to reach the camera. Motion blur during image acquisition is minimized by using a pulsed light source with an exposure time of approximately 1 ns.

In the current study, we evaluated the capability of this newly developed DIA apparatus (QicPic) using microcrystalline cellulose particles varying in particle size and shape. The repeatability and accuracy of the analysis was assessed systematically using single-component particle systems. The particle size and shape results obtained using the QicPic were compared with conventional laser diffraction result and scanning electron micrograph (SEM) images, respectively. The response of the QicPic to composition variations in binary mixtures containing spherical and rod-shape MCC particles were evaluated quantitatively.

2. Experimental

2.1. Materials

Four grades of microcrystalline cellulose particles obtained from Asahi Kasei chemicals (Tokyo, Japan) were used for this study. The Celphere™ MCC particles, including the CP-102, CP-305 and CP-708 grades, were relatively spherical but differed in particle size. The Ceolus™ KG-1000 MCC particles were rod-shaped with varying aspect ratios. The scanning electron micrograph images (Fig. 1a–d) show the detailed morphology of all the materials. All samples were used as received. True densities of the Ceolus™ KG-1000 and Celphere™ CP-102 materials were determined using a Helium pycnometer (Micromeritics, AccuPyc 1330, Norcross, GA, USA), and were found to be 1.53 g/ml and 1.52 g/ml, respectively.

2.2. Instrumentation

The newly developed QicPic DIA apparatus (Sympatec Inc., Clausthal-Zellerfeld, Germany) with Windox 5.0 software was used in the current study. The QicPic uses rear illumination with a visible pulsed light source that has an exposure time of 1 ns to minimize motion blur. The flash rate of the light source is adjustable from 1 to 500 Hz, and is synchronized with the high-speed camera that operates up to 500 frames per second. Dry powders are fed into the high-speed dry-sample disperser where they are accelerated to a speed of up to 100 m/s via a Venturi tube located in the dispersing

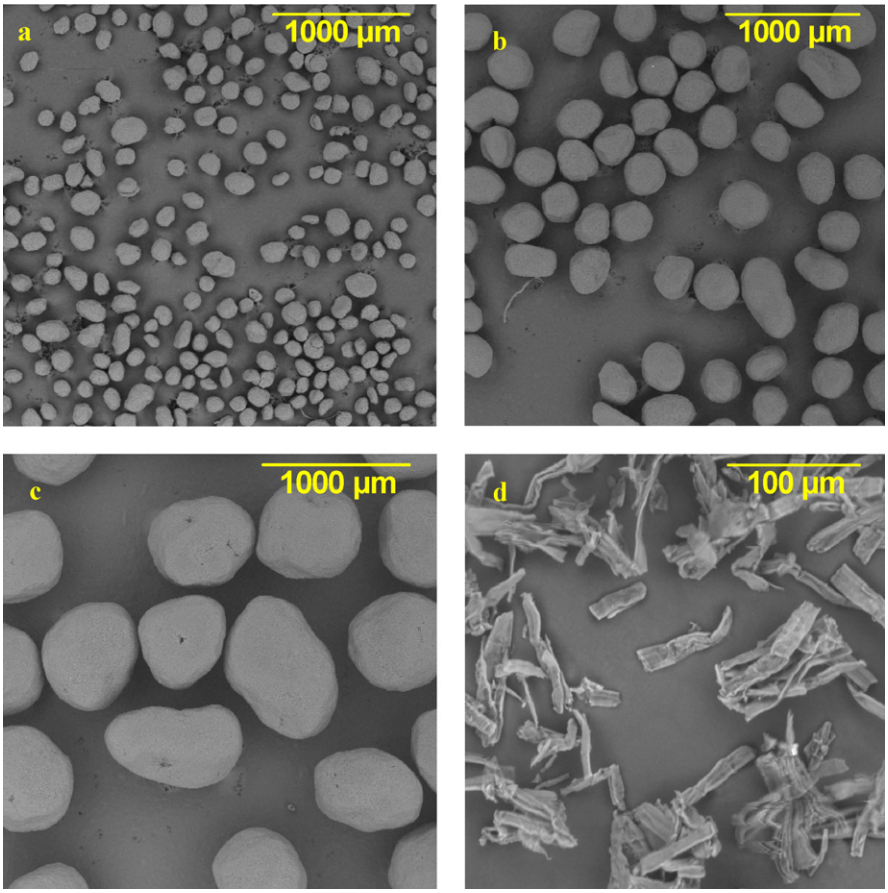

Fig. 1. SEM of the four excipients studied: (a) Celphere™ CP-102, (b) Celphere™ CP-305, (c) Celphere™ CP-708 and (d) Celous™ KG-1000.

line. During this process, dry powders are dispersed and aerosolized by particle–particle, particle–wall collisions and centrifugal forces caused by velocity gradients. Upon exit, particles enter the measurement zone decelerated and are finally collected by a Nilfisk™ vacuum system (Nilfisk-Advance A/S, Sognevej, Denmark). In a typical experiment, at least 10^5 particle images are captured by the camera and processed using appropriate image analysis algorithms included in the Windox 5.0 software.

A Sympatec HELOS (Helium–Neon Laser Optical System, Sympatec Inc., Clausthal-Zellerfeld, Germany) laser diffraction instrument with the same sample dispersing system as the QicPic was used to conduct particle size analysis for comparison purposes. A scanning electron microscope (Aspex Corporation, Delmont, PA, USA) was used to examine particle morphologies, and a micro-spinning riffler (Quantachrome Instruments, FL, USA) was used for subdividing bulk samples.

2.3. Experiments

For each QicPic measurement, approximately 5 ml of the MCC samples were obtained by subdividing the bulk material using a micro-spinning riffler to minimize sampling error. Instrument parameters, including sample feed rate, dispersing air pressure and frame rate, were evaluated with each sample during preliminary experiments. The optical concentration was kept below 1.5% to minimizing overlapping particles. The binary particle systems composed of Celphere™ CP-102 and Ceolus™ KG-1000 were prepared by weighing out appropriate amount of each component into a glass vial, and the powders were mixed thoroughly before analysis. The number of particle images captured during the QicPic measurements was kept above 10^5 to minimize potential statistical and sampling errors (Masuda and Iinoya, 1971).

Similar to the QicPic measurement, about 5 ml of the MCC samples, subdivided using the micro-spinning riffler, were used for particle size analysis with the HELOS. The optical concentration for the HELOS measurements was kept within the range of 4–6% during each measurement. Optical concentration within this range was found to provide adequate signal to noise ratio without causing multiple light scattering (Köhler et al., 2007).

2.4. Data presentation

Image analysis measures primarily the contour of particles to obtain both particle size and shape results. Attempts have been made to use a single value to describe the particle size and particle shape of non-spherical particles (Meloy and Mani, 1986; Podczeck, 1997; Kwan et al., 1999; Langston and Jones, 2001; Wang, 2006). Standard size descriptors include the equivalent projected circle (EQPC) and Feret diameters. The EQPC is the diameter of a circle that has the same projected area as the actual particle. The maximal and minimal Feret diameters are respectively the longest and shortest distance between two tangents to the contour of the particle. A schematic illustration of the EQPC and the Feret diameters are given in Fig. 2. For spherical particles, EQPC = maximal Feret diameter = minimal Feret diameter = particle diameter. For non-spherical

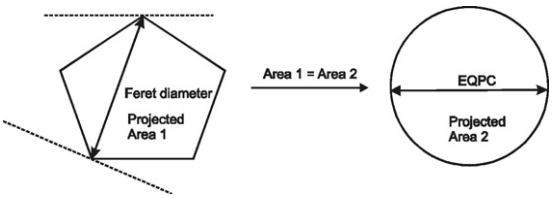

Fig. 2. Schematic illustration of the EQPC and Feret diameter.

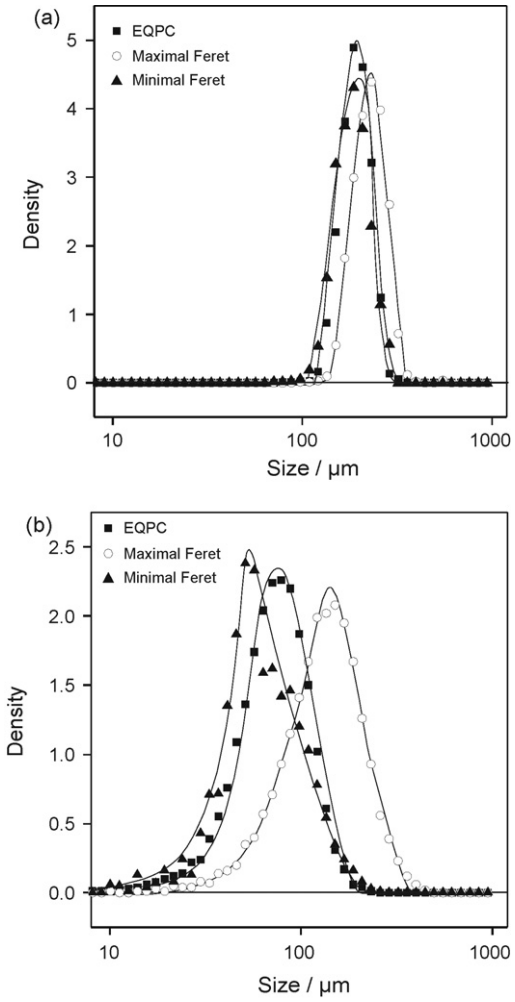

Fig. 3. Impact of size descriptor EQPC and Feret diameter on the particle size distribution of (a) spherical-shaped Celphere™ CP-102 and (b) rod-shaped Celous™ KG-1000 particles.

particles, the above relationship is not valid, and the selection of the evaluation method will impact the resulting particle size distribution. Fig. 3a and b shows the particle size distributions obtained with spherical (Celphere™ CP-102) and rod-shaped (Ceolus™ KG-1000) MCC particles using these different size descriptors. It is clear that the selection of size descriptor showed little impact on the particle size distribution of the spheres, whereas its impact on the distribution of rod-shaped particles was significant. Note the particle size distributions are illustrated in density instead of frequency. Expressing particle size distribution in density is a well-accepted and preferred method, as it eliminates the impact of the width of particle size interval on the form of the distribution (Sommer, 2001). The density in each size fraction is obtained by normalizing the frequency by the corresponding band-width. For the same reason, particle shape distributions are illustrated by density instead of frequency distributions as well.

Though a variety of shape factors have been proposed to describe the shape of non-spherical particles, it remains difficult to develop a general shape factor that would differentiate between all possible kinds of shapes (Podczeck, 1997; Hentschel and Page, 2003). Some of the standard shape factors include the aspect ratio and sphericity. Depending on the instrument manufacturer, the definition of these terms may vary. For the current study with the QicPic, sphericity is defined as the ratio between the perimeter of a circle that has the

same projected area as the particle to the measured perimeter, and is thus a value between 0 and 1. The aspect ratio is defined as the ratio of the minimal and maximal Feret diameter, and is thus also between 0 and 1. Based on these definitions, both sphericity and aspect ratio of a sphere equal to 1.

3. Results and discussion

3.1. Analysis repeatability

The repeatability of the QicPic measurements was evaluated using both the spherical (CP-102) and rod shaped (KG-1000) MCC particles. Six replicate measurements were conducted with each material using 0.5 bar sample dispersing pressure and 10–20% sample feed rate, and the particle size results are summarized in Table 1. The relative standard deviations of the 10th, 50th, and 90th percentile of the particle size distribution were calculated and were found to be less than 5%, indicating excellent method repeatability.

3.2. Comparison between the QicPic and HELOS

First, particle size results obtained with the QicPic and the conventional laser diffraction technique HELOS were compared using the spherical particles. The latter technique has been validated with various particle size standards and is widely accepted in the pharmaceutical industry for particle size characterization. If the optical setup and data processing algorithm used by the QicPic was appropriate, then the particle size distribution of the spherical samples obtained using the QicPic should agree well with that obtained from the HELOS (Xu, 2000; Xu et al., 2003). The particle size distribution reported by laser diffraction is the distribution of spherical particles with the same diffraction pattern as the measured particles (Köhler et al., 2007). For this reason, it was expected that the EQPC method would provide the best agreement with the laser diffraction data. It should also be noted that the particle size distributions obtained from the QicPic were presented in a volume-weighted fashion to be directly comparable to the HELOS data, which is by nature volume-weighted (Yu and Erickson, 2007). Fig. 4a shows the comparison results using the Celphere™ particles of various sizes. Overall, good agreement was observed between the QicPic and the HELOS results, indicating that the QicPic was able to provide accurate particle size distribution data. The only noticeable difference was with Celphere™ CP-102. The particle size distribution of CP-102 appeared to be coarser when analyzed using the QicPic than with the HELOS. The 90th percentile of the distributions (D90) were compared and showed that the D90 of CP-102 obtained from the QicPic was coarser than that obtained from the HELOS,

Table 1
Illustration of method repeatability with the DIA

Samples	Replicate	D10 (μm)	D50 (μm)	D90 (μm)
Celphere CP-102 (spherical)	1	167.8	219.3	280.6
	2	174.1	224.9	288.8
	3	172.7	225.7	280.8
	4	167.2	216.8	277.0
	5	173.2	227.1	289.6
	6	167.4	218.1	278.2
	RSD (%)	1.9	2.0	1.9
Ceolus KG-1000 (rod-shaped)	1	66.8	132.8	224.9
	2	69.8	141.5	245.4
	3	66.9	133.8	228.2
	4	67.1	133.4	225.2
	5	67.2	134.7	231.2
	6	67.9	137.0	235.2
	RSD (%)	1.7	2.4	3.3

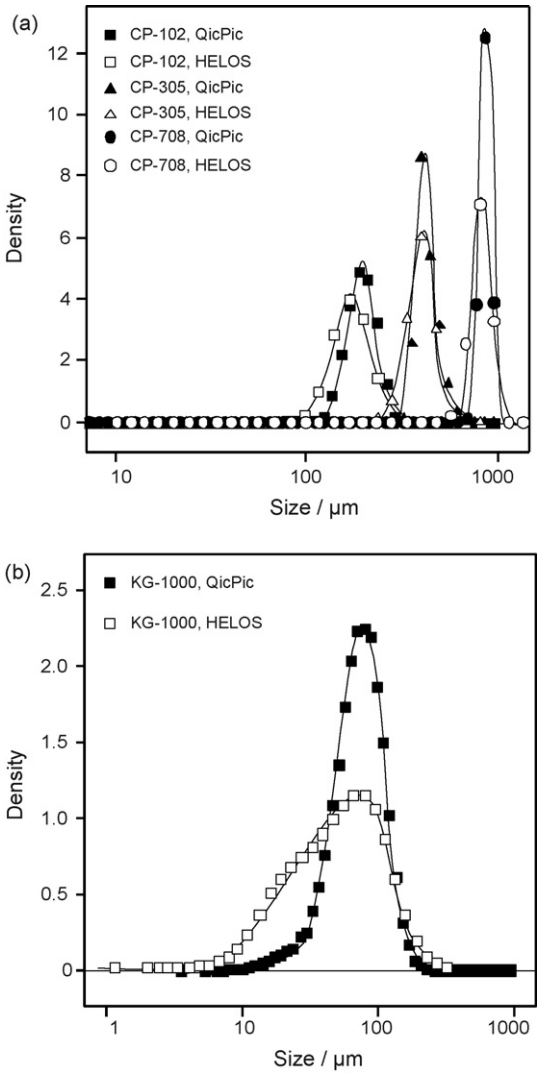

Fig. 4. Comparison of the particle size distributions obtained with the QicPic and HELOS using (a) Celphere™ CP-102, CP-305 and CP-708; (b) Celous™ KG-1000.

and the difference was statistically significant (*P*-value = 2.62E−07, ANOVA single factor). This was most likely due to a slight deviation of CP-102 particle shape from spherical, and this hypothesis was confirmed by the particle shape analysis (see later).

While the analysis of the spherical particles helped to cross-validate the instruments, the analysis of non-spherical particles revealed the intrinsic difference in the operating principles of the two techniques. The rod-shaped Ceolus™ KG-1000 was analyzed using both the QicPic and HELOS and the results were given in Fig. 4b. The particle size distribution obtained with the QicPic appeared to be much narrower than that obtained from the HELOS, with the coarse ends of the distributions overlapping. Previous studies have shown that laser diffraction tends to broaden the particle size distribution, and the phenomenon has been partially attributed to the data processing algorithms used and the preferred-orientation-effect associated with some instruments (Xu et al., 2003; Kelly and Kazanjian, 2006). Kelly and Kazanjian (2006) demonstrated the latter effect by analyzing rod-shaped mono-sized silicon dioxide particles with a laser diffraction particle size analyzer. Instead of obtaining a narrow size distribution (mono-sized), apparent bimodal distributions were observed with each mode corresponding to the breadth and length of the particle. Köhler et

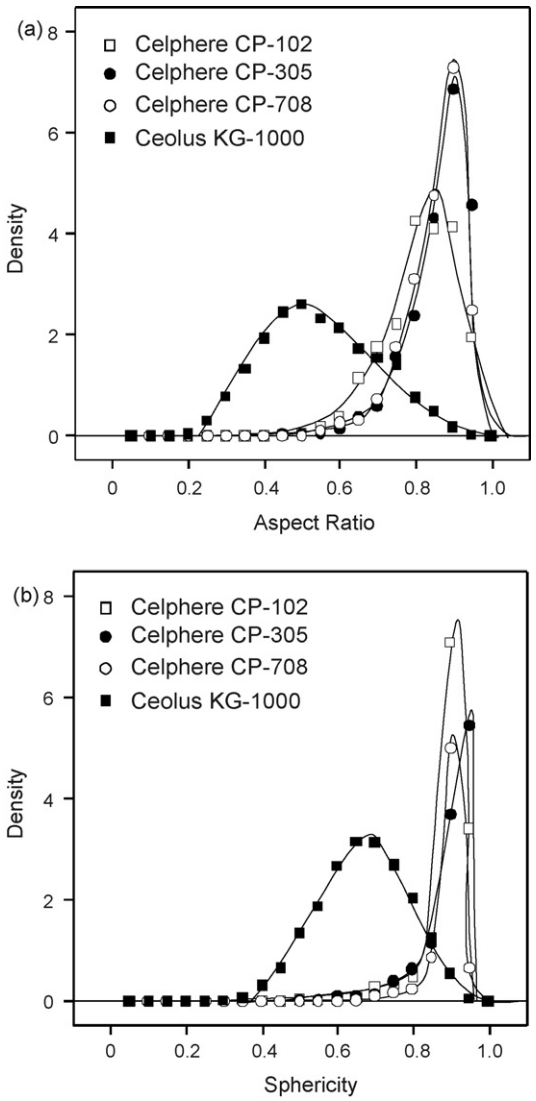

Fig. 5. (a) Aspect ratio distribution of Celphere™ CP-102, CP-305, CP-708 and Celous™ KG-1000; (b) Sphericity distribution of Celphere™ CP-102, CP-305, CP-708 and Celous™ KG-1000.

al. (2007) studied irregularly shaped silicon carbide particles with both the QicPic and HELOS and claimed that the difference observed between the two techniques was mainly due to particle shape effect on the evaluation procedure.

3.3. Particle shape analysis

The particle shape distribution of each single-component particle systems was evaluated with the QicPic, and the results were compared with the SEM micrographs (Fig. 1a–d). The particle shape was represented using both the aspect ratio and sphericity, and the results are given in Fig. 5a and b. Among the three spherical samples, CP-102 showed the broadest distribution in aspect ratio, indicating the most significant deviation from spherical (Fig. 5a). This result was consistent with the discrepancy observed between the QicPic and HELOS particle size data, and was confirmed qualitatively by the SEM micrographs (Fig. 1a). The aspect ratio distribution of Ceolus™ KG-1000 differed significantly from that of the Celphere™ particles, covering a broad range from 0.2 to 0.95. Comparison with the corresponding SEM micrograph revealed that while the majority of the KG-1000 particles has aspect ratios of less than 0.5, particle fragments present in the sample were more equant with higher aspect ratios, consistent with the broad distribution obtained using the QicPic.

The sphericity distributions were found to be very similar among the spherical samples, but differed significantly from that of the Ceolus™ KG-1000, which spanned a broad range from 0.4 to 0.9 (Fig. 5b). An attempt was made to relate the sphericity of the Ceolus™ KG-1000 to its aspect ratio. Assuming a rectangular projection, sphericity of a rod-shaped particle can be easily derived from its aspect ratio as shown below:

$$S = \frac{(n\pi)^{0.5}}{1+n}$$

where S is sphericity, and n is reciprocal of aspect ratio of the particle. Using the upper and lower limits of the aspect ratio distribution (0.2–0.95) led to a manually calculated range of sphericity of 0.66–0.89. To understand why the lower end of the measured sphericity (0.4) was smaller than the estimated sphericity (0.66), the SEM micrograph was consulted. The sphericity is defined as the ratio between the perimeters of an equivalent circle (circle with the same project area as actual particle) and the real particle, so any increase in particle perimeter without changing its projected area would lead to a decrease in sphericity. The SEM micrograph reveals that some KG-1000 particles were twisted and bent with rough surfaces and it is probable that this led to an increase in particle perimeter with little impact on the projected area. Consequently, the measured sphericity was smaller than that derived from the aspect ratio, which did not take into account these factors.

Overall, the data showed that the shape distributions obtained from the QicPic agreed with the SEM micrographs semi-quantitatively. While both the aspect ratio and sphericity could be used to differentiate between the spherical and rod-shaped particles, the aspect ratio appeared to be more sensitive in detecting small differences such as those presented among the spherical samples. Hence, in the subsequent studies the aspect ratio alone was used to quantify the particle shape.

3.4. Binary particle systems

The data presented so far has demonstrated that the QicPic is suitable for characterizing single-component systems with a variety of shapes. In this section, the DIA technique was challenged with a series of binary particulate systems composed of varying mass ratios of spherical and rod-shaped particles. The two components used were the Ceolus™ KG-1000 and Celphere™ CP-102 particles. The mass fraction of Ceolus™ KG-1000 was denoted as X_a and was varied systematically between 0 and 1. At $X_a = 0$ and 1, the system was composed of 100% Celphere™ CP-102 and Ceolus™ KG-1000, respectively. The number of particles measured in these experiments was approximately 10^7.

Fig. 6a shows an overlay of the particle size (EQPC) distributions obtained at varying mass fractions of Ceolus™ KG-1000, the lines shown in the graph are for eye-guide only. A mono-modal distribution was obtained at $X_a = 0$, reflecting the characteristic of Celphere™ CP-102. With an addition of 6% of the KG-1000, the distribution became bi-modal with a second peak apparent on the left. With further addition of KG-1000, the location of the modes remained constant and the height of the peaks responded to the controlled changes in the composition. As X_a increased to 1, the mono-modal distribution was recovered reflecting the property of the KG-1000 sample. It was noticed that the particle size distribution responded to the composition change more sensitively when the X_a was small. For instance, notable change in the distributions was observed when X_a was increased from 0 to 0.06

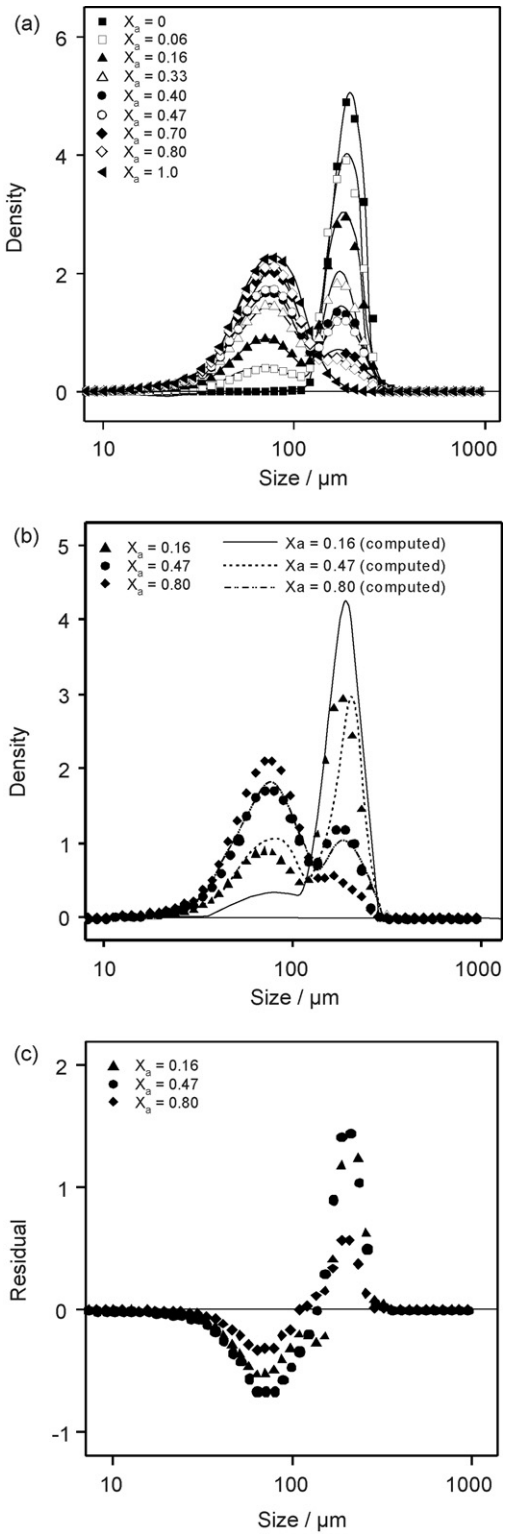

Fig. 6. (a) Overlay of the particle size (EQPC) distributions obtained in CP-102/KG-1000 binary particle systems with varying mass fractions of KG-1000 (denoted as X_a); (b) comparison of the computed and measured particle size distributions of the mixture samples with varying compositions; (c) residual analysis between the computed and measured distributions.

(demonstrated by the filled and open squares in Fig. 6a). However, when X_a was increased from 0.4 to 0.47, the corresponding distributions shifted only slightly (demonstrated by the filled and open circles in Fig. 6a). The observation seemed to indicate that the QicPic did not respond linearly to the variation in the sample composition. For further analysis, the measured particle size distributions were compared against the computed distributions of the mixture samples. The computed distributions of the mixture samples were obtained by summing the distributions of the pure materials (KG-1000 and CP-100) weighted by their respective mass fractions in the mixtures. Distributions of three mixtures with X_a equals to 0.16, 0.47 and 0.80 were computed and overlaid with the corresponding measured distributions, and were shown in Fig. 6b. The computed distributions were demonstrated with lines and the measured distributions with individual symbols for the ease of eyes. Apparent discrepancies were present between the measured and computed distributions of the three mixture systems analyzed. Residuals between the measured and the computed distributions (residual = computed density – measured density) were plotted against the particle size in Fig. 6c. The residuals obtained with the three mixture systems showed similar patterns with negative values at small particle size and positive values at large particle size. Since the peak at the small particle size range reflected the presence of KG-1000, the data in Fig. 6b and c appeared to indicate that the QicPic overestimated the amount of KG-1000 particles present in the mixture samples.

Aspect ratio distributions of the above binary systems were also measured, and the results are given in Fig. 7a. The aspect ratio distribution obtained at $X_a = 0$ covered a range from 0.45 to 1.0, corresponding to the characteristics of Celphere^{TM} CP-102. With the addition of 6% of KG-1000, the distribution broadened by extending its lower limit to about 0.2. At $X_a = 0.16$, the distribution became bi-modal with a second peak merging from the left hand side. Further increases in the mass fraction of KG-1000 led to continuous growth of this second peak and the decrease of the first peak. A mono-modal distribution was recovered after X_a reached 1. The aspect ratio distributions of three mixture samples ($X_a = 0.16$, 0.47 and 0.80) were computed by summing the distributions of the pure materials weighted by their respective mass fractions in the mixtures. The computed distributions were overlaid with the measured distributions (Fig. 7b) and the residuals between each pair of distributions were plotted against the aspect ratio (residual = computed density – measured density) (Fig. 7c). Discrepancies between the computed and measured aspect ratio distributions, similar to those observed in the particle size distributions, were present. Residuals were negative at small aspect ratio values and positive as aspect ratio approached 1. Since the small aspect ratio values reflected the presence of KG-1000, the data again appeared to indicate that the QicPic overestimated the amount of KG-1000 material in the mixtures.

It was suspected that the observed discrepancies between the measured and the computed distributions were due to a particle porosity effect. While the measured particle size and particle shape distributions were both volume-weighted, the computed distributions of the binary mixtures were obtained using the mass fractions of the pure components in the mixtures. The mass fractions were used because of the similar true densities of the KG-1000 (1.53 g/ml) and CP-100 (1.52 g/ml) materials. However, additional insights gained from the SEM images indicated that using the true density may not have correctly reflected the actual volume fractions occupied by the KG-1000 particles in the mixtures at the given mass fractions (Fig. 1). The SEM pictures revealed that the KG-1000 particles were tube-like with hollow interiors. For a given mass, the volume occupied by the exterior of such particles could be much larger than that estimated using the true density (1.53 g/ml).

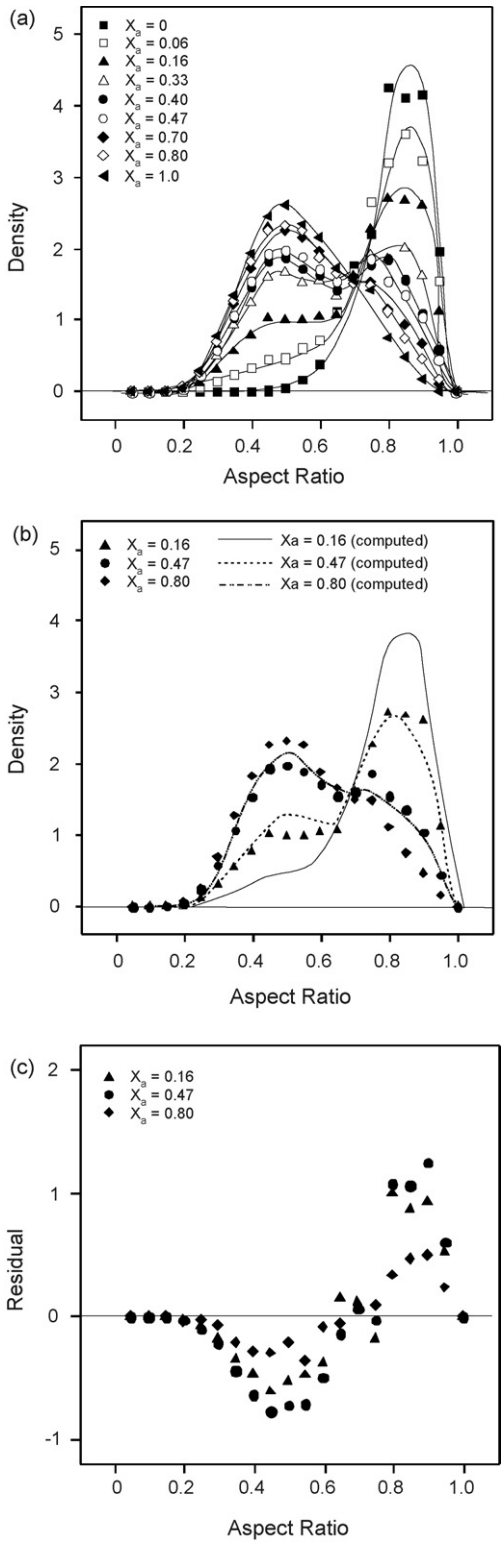

Fig. 7. (a) Overlay of the aspect ratio distributions obtained in CP-102/KG-1000 binary particle systems with varying mass fractions of KG-1000 (denoted as X_a); (b) comparison of the computed and measured aspect ratio distributions of the mixture samples with varying compositions; (c) residual analysis between the computed and measured distributions.

In other words, the apparent volume fraction of the KG-1000 in a binary mixture could be (much) higher than that calculated using its true density. Further analysis revealed that excellent agreement could be achieved between the computed and the measured particle size and shape distributions with various X_a values when the volume fraction of the KG-1000 was estimated using an apparent density of 0.44 g/ml. Note this value was found to be close to the tapped density of KG-1000 (0.30 g/ml), which reflected the presence of porosity in the material. Additional studies with materials of different porosities, morphologies and particle sizes may be needed to further confirm this hypothesis.

4. Conclusions

The capability of the newly developed dynamic image analysis instrument QicPic equipped with the high-speed dry-powder-dispersing device was investigated systematically using various MCC particles. Method repeatability was first evaluated by analyzing both spherical and rod-shaped particles. Secondly, instrument cross-validation was conducted by comparing the particle size distribution of spherical particles obtained with the QicPic and with a conventional laser diffraction instrument (HELOS). While good agreement was observed with spherical particles, significant differences were found when analyzing rod-shaped Ceolus™ KG-1000 particles, revealing the intrinsic difference in operating principles between these two techniques. Thirdly, particle shape distributions of several spherical and rod-shaped samples obtained with the QicPic were compared to SEM micrographs, and semi-quantitative agreement was obtained. Lastly, the QicPic system was challenged with a series of binary particulate systems composed of both spherical (CP-102) and rod-shaped (KG-1000) particles of varying mass ratios. The particle size and particle shape distributions of these binary mixtures were computed using the distributions of the pure components weighted by their respective mass fractions. It was found that the QicPic appeared to overestimate the amount of the KG-1000 particles present in all the mixtures. Further analysis indicated that due to the hollow interior of the KG-1000 material, the actual volume occupied by the exterior of such particles could be (much) larger than that estimated using its true density. It was found that when an apparent density of 0.44 g/ml was used for estimating the volume fraction of KG-1000, excellent agreement between the measured and the computed distributions could be obtained for the mixture samples.

It is expected that the capability of the QicPic to simultaneously measure particle size and shape could help to provide valuable insights into a variety of pharmaceutical processes where changes in particle size and shape are often coupled. For instance, such analysis could be used to understand the impact of particle size and shape on powder mixing and segregation, so that excipients with suitable size and shape could be selected to improve powder-blending efficiency or minimize potential segregations.

Acknowledgement

The authors gratefully thank Dr. Ilie Saracovan for conducting the SEM analyses, and Dr. Norma Leyva for insightful discussions on statistical analysis.

References

Bao, N., Shen, L., Feng, X., Lu, X., Yanagisawa, K., 2004. Shape and size characterization of potassium titanate fibers by image analysis. J. Mater. Sci. 39, 469–476.

Deriemaeker, L., Finsy, R., 2005. Shape and size determination by laser diffraction: average aspect ratio and size distribution by volume; feasibility of data analysis by neural network. Part. Part. Syst. Charact. 22, 5–13.

Fee, J.P.H., Collier, P.S., Launchbury, A.P., Clarke, R.S.J., 1992. The influence of particle size on the bioavailability of inhaled temazepam. Br. J. Clin. Pharm. 33, 641–644.
Hentschel, Mark L., Page, Neil W., 2003. Selection of descriptors for particle shape characterization. Part. Part. Sys. Charact. 20, 25–38.
Hintz, R.J., Johnson, K.C., 1989. The effect of particle size distribution on dissolution rate and oral absorption. Int. J. Pharm. 51, 9–17.
Jillavenkatesa, A., Dapkunas, S.J., Lum, L.-S.H., 2001. Particle Size Characterization. U.S. Government Printing Office, Washington.
Johnson, K.C., Swindell, A.C., 1996. Guidance in the setting of drug particle size specifications to minimize variability in absorption. Pharm. Res. 13, 1795–1798.
Kelly, R.N., Kazanjian, J., 2006. Commercial reference shape standards use in the study of particle shape effect on laser diffraction particle size analysis. AAPS Pharm. Sci. Tech. 7, Article 49, 7, E1–E12.
Köhler, U., List, J., Witt, W., 2007. Comparison of Laser Diffraction and Image Analysis under Identical Dispersing Conditions. Partec, Nürnberg.
Kwan, A.K.H., Mora, C.F., Chan, H.C., 1999. Particle shape analysis of coarse aggregates using digital image process. Cement Concrete Res. 29, 1403–1410.
Langston, P.A., Jones, T.F., 2001. Non-spherical 2-dimensional particle size analysis from chord measurements using Bayes' theorem. Part. Part. Syst. Charact. 18, 12–21.
Li, M., Wilkinson, D., Patchigolla, K., 2005. Comparison of particle size distributions measured using different techniques. Particul. Sci. Technol. 23, 265–284.
Ma, Z., Merkus, H.G., Scarlett, B., 2001. Extending laser diffraction for particle shape characterization: technical aspects and application. Powder Technol. 118, 180–187.
Massol-Chaudeur, S., Berthiaux, H., Dodds, J.A., 2002. Experimental study of the mixing kinetics of binary pharmaceutical powder mixtures in a laboratory hoop mixer. Chem. Eng. Sci. 57, 4053–4065.
Masuda, H., Iinoya, K., 1971. Theoretical study of the scatter of experimental data due to particle-size-distribution. J. Chem. Eng. Jpn. 4, 60–66.
Meloy, T.P., Mani, B.P., 1986. Particle shape analysis and separation techniques: a critical review. J. Powder Bulk Solids Technol. 10, 15–20.
Mullarney, M.P., Hancock, B.C., Carlson, G.T., Ladipo, D.D., Langdon, B.A., 2003. The powder flow and compact mechanical properties of sucrose and three high-intensity sweeteners used in chewable tablets. Int. J. Pharm. 257, 227–236.
Podczeck, F., 1997. A shape factor to assess the shape of particles using image analysis. Powder Technol. 93, 47–53.
Podczeck, F., Sharma, M., 1996. The influence of particle size and shape of components of binary powder mixtures on the maximum volume reduction due to packing. Int. J. Pharm. 137, 41–47.
Rabinski, G., Thomas, D., 2004. Dynamic digital image analysis: emerging technology for particle characterization. Water Sci. Technol. 50, 19–26.
Shah, K.R., Badawy, S.I.F., Szemraj, M.M., Gray, D.B., Hussain, M.A., 2007. Assessment of segregation potential of powder blends. Pharm. Dev. Technol. 12, 457–462.
Sommer, K., 2001. 40 years of presentation particle size distribution—yet still incorrect? Part. Part. Syst. Charact. 18, 22–25.
Swaminathan, V., Kildsig, D.O., 2002. Polydisperse powder mixtures: effect of particle size and shape on mixture stability. Drug Dev. Ind. Pharm. 28, 41–48.
Wang, W., 2006. Image analysis of particles by modified Ferret method—best-fit rectangle. Powder Technol. 165, 1–10.
Witt, W., Köhler, U., List, J., 2004. Direct Imaging of Very Fast Particles Opens the Application of the Powerful (Dry) Dispersion for Size and Shape Characterization. Partec, Nürnberg.
Witt, W., Köhler, U., List, J., 2005. Experiences with dry dispersion and high-speed image analysis for size and shape characterization. Particulate Systems Analysis, Stratford-upon-Avon, UK.
Xu, R., 2000. Particle Characterization: Light Scattering Methods. Kluwer Academic Publishers, Norwell.
Xu, R., Andreina, O., Guida, D., 2003. Comparison of sizing small particles using different technologies. Powder Technol. 132, 145–153.
Yin, S.X., Franchini, M., Chen, J., Hsieh, A., Jen, S., Lee, T., Hussain, M., Smith, R., 2005. Bioavailability enhancement of a COX-2 inhibitor, BMS-347070, from a nanocrystalline dispersion prepared by spray-drying. J. Pharm. Sci. 94, 1598–1607.
Yu, W., Erickson, K., 2007. Chord length characterization using focused beam reflectance measurement probe—methodologies and pitfalls. Powder Technol. 185, 24–30.
Zhang, Y., Johnson, K.C., 1997. Effect of drug particle size on content uniformity of low-dose solid dosage forms. Int. J. Pharm. 154, 179–183.